ACS OMEGA

Open Access

This article is licensed under CC-BY-NC-ND 4.0

http://pubs.acs.org/journal/acsodf

Article

MeCP2-Induced Alternations of Transcript Levels and m6A Methylation in Human Retinal Pigment Epithelium Cells

Xueru Zhao, Yongya Zhang, Fei Wu, Xue Li, Sibei Guo, and Xiaohua Li*

Cite This: *ACS Omega* 2023, 8, 47964−47973

Read Online

ACCESS | Metrics & More | Article Recommendations | Supporting Information

ABSTRACT: MeCP2 is a transcriptional regulator that is involved in epithelial-mesenchymal transition (EMT) and is highly expressed in proliferative vitreoretinopathy. m6A methylation is a critical post-transcriptional regulation in eukaryotic cells. However, the connection between MeCP2 and m6A methylation has not been revealed in retinal pigment epithelium (RPE), and the regulatory role of MeCP2 at the post-transcriptional level in an m6A-dependent manner is rarely investigated. In this study, we used sequencing to reveal differences in transcript levels and m6A abundance of individual genes in RPE cells after treatment with human recombinant protein MeCP2. The biological functions and processes of differential genes were further analyzed by bioinformatics. The results exhibited that after MeCP2 treatment, 65 genes were up-regulated and 43 genes were down-regulated at the transcription level, and 4 peaks were hypermethylated and 9,041 peaks were hypomethylated at the m6A modification level. Enrichment analysis found that differentially expressed genes were associated with organic acid metabolism, melanogenesis, and vascular smooth muscle contraction. In addition, differentially methylated genes were related to cell junction, RNA processing and metabolism, cell activity, actin cytoskeleton, and several signaling pathways associated with EMT. Further conjoint analysis indicated that the transcription and m6A levels of the *EGR1*, *ELOVL2*, and *SFR1* genes were altered, and EGR1 is an essential transcription factor in the EMT process. The RNA levels and m6A levels of the three genes were verified by qPCR and m6A-IP-qPCR, respectively. Overall, this study preliminarily revealed the differential mapping of MeCP2-induced m6A modifications, which contributes to the study of the epigenetic and EMT mechanism in RPE cells.

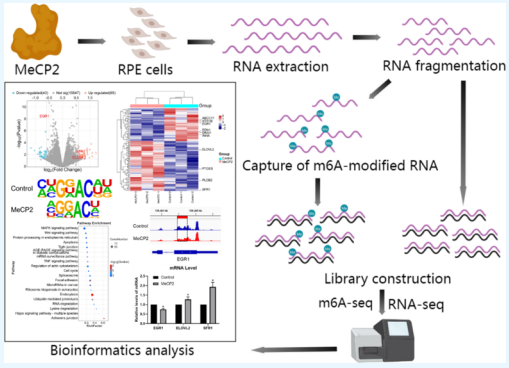

1. INTRODUCTION

Retinal pigment epithelium (RPE) cells, which play a critical role in diverse retinal diseases, are a highly polar array of quiescent cells and are closely attached to the choroidal layer.[1] However, RPE cells will undergo the EMT process, which is characterized by upregulation of mesenchymal markers and enhanced cell migration and proliferation after stimulation with cytokines and growth factors.[1] Numerous studies have shown that RPE cells undergoing the EMT process contributes to the formation of fibrous membranes.[1,2] By immunohistochemical labeling of the proliferative vitreoretinopathy (PVR) membrane, it was found that the membranes contained glial cells and RPE cell populations, among which RPE cells were considered to exist stably in PVR membranes.[3] In addition, RPE cells could undergo the EMT process by inducers under culture conditions, and general inducers mainly include transforming growth factor β (TGF-β) and tumor necrosis factor α (TNF-α).[4] The EMT process of RPE cells is complex and might be induced by multiple factors or signaling pathways. Therefore, elucidating the EMT mechanism in RPE cells is conducive to the defense and treatment of retinal diseases.

Epigenetics such as DNA and RNA methylation are involved in the regulation of gene expression and are associated with the development of the EMT process. m6A methylation is the most abundant internal modification of RNA, which play an essential roles in the post-transcriptional regulation of RNA.[5] The regulatory mechanism of m6A methylation are controlled by methyltransferases, demethylases, and methylation binding proteins.[6] Among them, methyltransferase METTL3 has been confirmed to play an inhibitory role in PVR membrane formation and the EMT process, and overexpression of METTL3 can attenuate TGF-β1-induced EMT through the wnt/β-catenin pathway in human RPE cells,[7] suggesting an inhibitory effect of METTL3 on EMT. However, a recent study came up with the opposite result. METTL3 was up-regulated in mouse subretinal fibrotic RPE cells, and

Received: September 2, 2023
Revised: November 5, 2023
Accepted: November 20, 2023
Published: December 5, 2023

© 2023 The Authors. Published by American Chemical Society

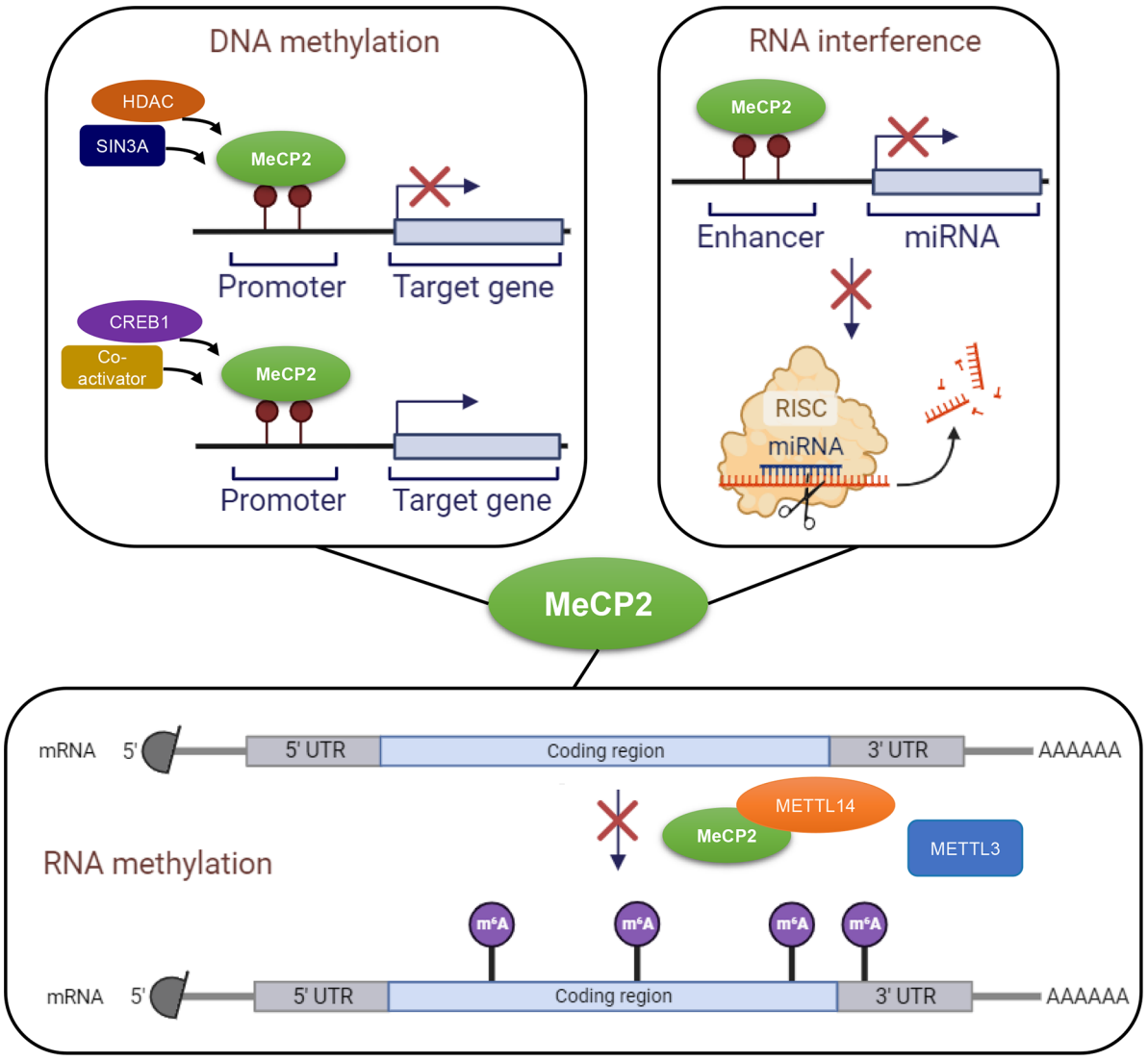

Figure 1. Schematic diagram of the MeCP2 function in epigenetics. MeCP2 has diverse functions in epigenetics. During DNA methylation, MeCP2 binds to the promoter of the target gene and represses or activates gene transcription. Similarly, in RNA interference, MeCP2 affects the transcription of certain miRNAs. During RNA methylation, MeCP2 competitively binds to the methyltransferase METTL14 and affects m6A modification, thereby impacting gene expression. Diagram constructed by BioRender.

knockdown of METTL3 can reduce the degree of retinal fibrosis; in addition, it was confirmed that high-mobility group AT-hook 2 (HMGA2) was a modification target of METTL3, which activates the EMT key transcription factor SNAIL.[8] This suggests that even within the same cell type (RPE cells), the regulatory mechanism of m6A may be different in different species. Moreover, with the rapid advances in sequencing technology, the transcriptome-wide modification profile of m6A methylation has been revealed, and it was found that m6A methylation might be involved in the regulation of a variety of biological processes.[9] The modification profile of m6A has been extensively studied in multifarious cells; however, studies on m6A methylation modification profiles in RPE cells are still relatively lacking, and the biological functions of m6A in RPE cells are largely unknown.

MeCP2 is identified as a global transcriptional repressor and consists of 486 amino acids, which contains a methylated DNA binding domain (MBD) that preferentially recognizes and binds methylated CpGs sequences as well as a C-terminal transcription repression domain (TRD) that inhibits transcriptional activity.[10] MeCP2 plays an important role in DNA methylation, RNA interference, and RNA methylation and is able to directly bind to methylation-modified DNA to affect the transcription of target genes or miRNAs, as well as to the methyltransferase METTL14 to affect m6A modification (Figure 1).[11−13] MeCP2 also forms complexes with histone deacetylases (HDACs) and SIN3 transcription regulator family member A (SIN3A) to further inhibit gene transcription in combination with histone acetylation modifications.[14] In addition, MeCP2 associates with transcriptional activator CREB1 to activate gene transcription.[15] Mutations in MeCP2 are known to cause RTT syndrome, which is defined as a serious neurodevelopmental disease.[16] MeCP2 is also associated with varieties of cancers, such as breast, lung, and prostate cancer. MeCP2 acts as a cancer suppressor in some cancer cells. For example, in breast cancer cells, MeCP2 represses gene expression by binding to methylation sites in the promoter region of the susceptibility gene BRCA1[11] or inhibition of tumor cell proliferation and migration by promoting the expression of epithelial markers.[17] However,

https://doi.org/10.1021/acsomega.3c06610
ACS Omega 2023, 8, 47964−47973

MeCP2 promotes tumorigenesis and the EMT program in some cell types. In pancreatic cancer, MeCP2 expression is up-regulated and promotes EMT by activating TGF-β1, accompanied by increased expression of mesenchymal markers including vimentin, N-cadherin, and SNAIL.[18]

In addition, the function of MeCP2 in RPE cells has also been investigated. Studies showed that MeCP2 is highly expressed in the PVR membranes and inhibition of MeCP2 function, including DNA methylation inhibitor treatment and knockdown of MeCP2 gene, resulting in decreased mesenchymal markers (α-SMA and fibronectin) in RPE cells.[19] Furthermore, our previous study found that the expression of α-SMA was significantly up-regulated after human recombinant protein MeCP2 treated RPE cells for 72 h.[20] This suggests that MeCP2 plays a role in EMT of RPE cells; however, the current studies on MeCP2 tend to focus on pretranscriptional regulation, and it is unclear whether MeCP2 can alter the m6A status of mRNAs in RPE cells. Based on the effect of MeCP2 on EMT of RPE cells, we determined the changes in the transcription level and m6A abundance of individual gene by high-throughput sequencing, which revealed the m6A modification profile in RPE cells with and without MeCP2 treatment. Moreover, this study is expected to discover MeCP2-induced alternations in the m6A regulatory network in RPE cells, which will contribute to the disclosure of new molecular targets for the EMT mechanism.

2. MATERIALS AND METHODS

2.1. Cell Lines and MeCP2 Treatment. Human hTERT RPE-1 (ATCC) cells were cultured in DMEM/F12 medium (Solarbio) with 10% fetal bovine serum (FBS, Gibco) and 0.01 mg/mL of hygromycin B (Solarbio). The next day, they were placed in a fresh DMEM/F12 medium (1% FBS). Twenty ng/mL human recombinant protein MeCP2 (Abcam) was added to the treatment group, and an equal volume of phosphate buffered solution (PBS) was added to the control group. hTERT RPE-1 cells were cultured in a 37 °C cell incubator for 72 h. Three parallel samples were set per group.

2.2. RNA Isolation. After washing the cells three times with sterile PBS, 1 mL of TRIzol reagent (Takara) was added, and cells were lysed for 5 min on ice. Cell lysate was transferred to a sterile enzyme-free centrifuge tube, and 200 μL of chloroform was added to isolate RNA. The supernatant was transferred to a new centrifuge tube, and an equal volume of isopropanol was added to precipitate RNA. After washing with 75% ethanol, the RNA was dissolved in sterile enzyme-free water. Subsequent DNA digestion was carried out with DNaseI (Takara). Total RNA was used for sequencing after the quality and concentration of RNA was determined.

2.3. Library Construction and Sequencing. Sequencing and analysis were performed by Seqhealth Technology Co., Ltd. (Wuhan). For m6A-seq, the mRNA was enriched with oligo d(T) magnetic beads (VAHTS) and then broken into short fragments of about 100 bp with divalent cations.[21] The fragmented mRNA was divided into two groups: the input group and IP group, respectively. The IP group was subsequently coimmunoprecipitated with m6A antibody (Synaptic Systems). The library was constructed with a Stranded mRNA-seq Library Prep Kit (HealthSeq), enriched and quantified, and finally sequenced on a Novaseq sequencer (Illumina).[22] For RNA-seq, the m6A enrichment process was omitted. Raw data from sequencing have been uploaded to the SRA database (SRA accession: SRP470199, Bioproject: PRJNA1035791).

2.4. Sequencing Data Analysis. The raw data were filtered with Trimmomatic to obtain high-quality clean data.[23] Subsequently, the deduplicated data were mapped to the reference genome *Homo sapiens* GRCh38 with the STAR tool (https://github.com/alexdobin/STAR) to obtain comprehensive transcriptional information. Peak calling and peak annotation were performed using exomePeak[24] and bedtools (https://github.com/arq5x/bedtools), respectively. The analysis of peak distribution was performed using deepTools,[25] and the m6A motif analysis was implemented by Homer software.[26] RPKM (reads per kilobase per million reads) value was used to assess gene expression levels, and edgeR package was used to identify differentially expressed genes between groups.[27]

2.5. Functional Analysis and Plotting. Differential genes were selected based on fold changes and *p*-value/FDR. Annotated differential genes were subjected to functional analysis using Gene Ontology (GO) and Kyoto Encyclopedia of Genes and Genomes (KEGG) through the OmicShare platform, with FDR less than 0.05 indicating statistical significance.[28] The PCA, volcano, and nine-quadrant diagrams were made by OmicShare tools, and IGV plots were drawn by the Itegrative Genomics Viewer software.[29]

2.6. qPCR. First, RNA was reverse transcribed into cDNA using the reverse transcription kit (Takara). Next, the reaction system was prepared, and the reaction program was set up according to the instructions of the real-time quantitative PCR kit (Takara). *GAPDH* gene was set as the reference gene, and the expression levels of *EGR1*, *ELOVL2*, and *SFR1* genes were detected. The primers used are as follows: GAPDH-F: 5′-ATCCCATCACCATCTTCCAGG-3′; GAPDH-R: 5′-GATGACCCTTTTGGCTCCC-3′; EGR1-F: 5′-CACCTGACCGCAGAGTCTTTT-3′; EGR1-R: 5′-CACTAGGCCACTGACCAAGCT-3′; ELOVL2-F: 5′-GCTCTCAATATGGCTGGGTAAC-3′; ELOVL2-R: 5′-AGTTGTAGCCTCCTTCCCAAGT-3′; SFR1-F: 5′-CCTCTGCGAATCCATCATCTC-3′; SFR1-R: 5′-CCTCTGTGGAAGATGCTGGTT-3′.

2.7. m6A-IP. m6A-modified mRNA fragments were enriched by the m6A methylated fragment enrichment kit (EpiQuik), and the specific operations were as follows: 10 μg of RNA for the IP group and 400 ng for the Input group. First, the immunocapture solution was configured in which RNA was incubated with m6A antibody or IgG antibody for 90 min at room temperature. The RNA was fragmented, digested, and released by proteases. Finally, RNA was captured using magnetic beads, and after the magnetic beads were washed three times, RNA was lysed in 13 μL of DNase/RNase-free water. The enriched RNA was subsequently subjected to reverse transcription and qPCR.

2.8. Western Blot. Total protein was extracted using 100 μL of RIPA lysate (1% PMSF). Loading buffer was added, and proteins were denatured, followed by SDS-PAGE electrophoresis. The proteins were then transferred to a PVDF membrane and incubated in 3% bovine serum albumin for 2 h. MeCP2 (CST) or GAPDH (Proteintech) specific antibody was added, and the mixture was incubated at 4 °C overnight. After adding the appropriate secondary antibody and incubating for 1 h, the protein was finally exposed using the ECL Reagent (Millipore).

https://doi.org/10.1021/acsomega.3c06610
ACS Omega 2023, 8, 47964−47973

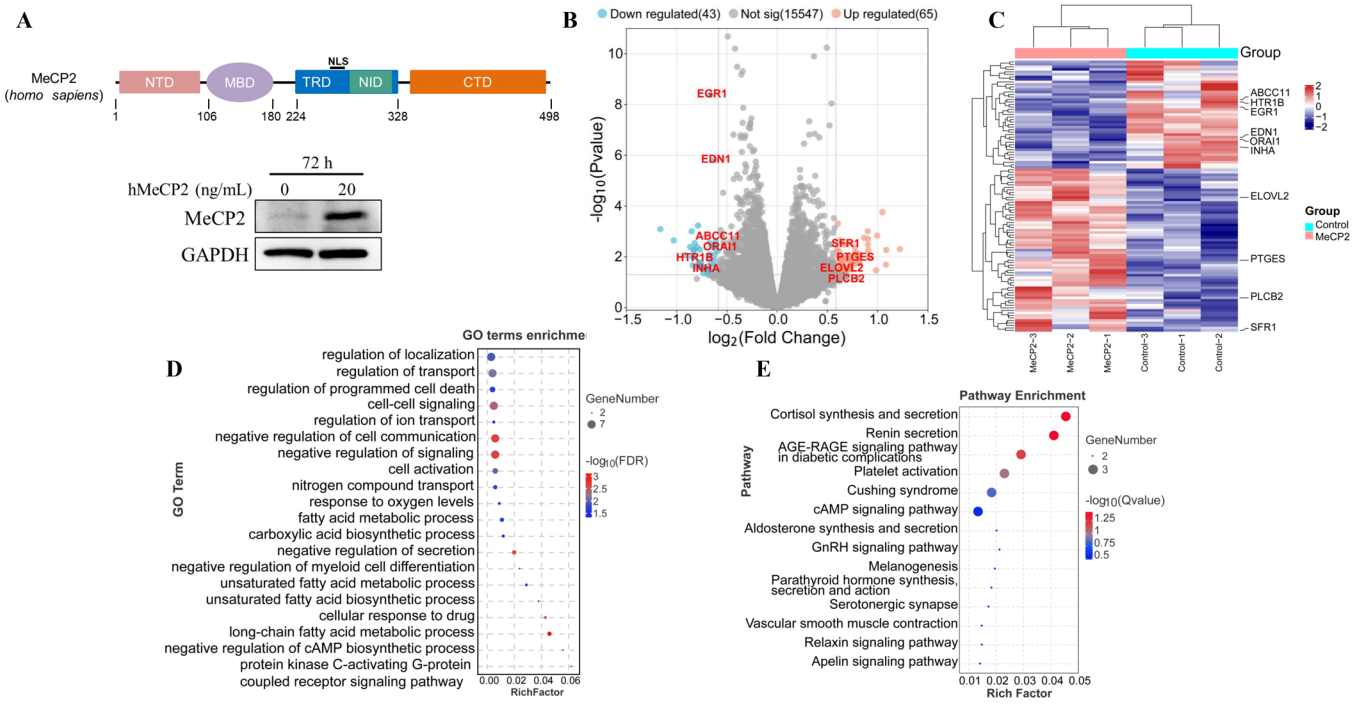

Figure 2. MeCP2-induced changes in gene expression in hTERT RPE-1 cells. (A) Domain of human MeCP2 protein and detection of intracellular MeCP2 levels. The top is the domain of human MeCP2. NTD: N-terminus domain; MBP: methylated-DNA binding domain; TRD: transcription repression domain; NLS: nuclear localization domain; NID: Ncor1-interacting domain; CTD: C-terminal domain. The bottom is the MeCP2 protein level. Intracellular MeCP2 protein levels in RPE cells treated with 20 ng/mL MeCP2 for 72 h were detected by Western blot. (B) Volcano plot of DEGs. Each dot represents a gene, red dots mean hyper-expressed genes, blue dots mean hypo-expressed genes, and gray dots mean genes without difference. (C) Heatmap analysis of DEGs. GO enrichment (D) and KEGG enrichment (E) of DEGs.

3. RESULTS

3.1. Differentially Expressed Genes (DEGs) Induced by MeCP2 in hTERT RPE-1 Cells. MeCP2 is a binding protein of methylated DNA as well as a transcriptional repressor that consists of two important structural domains: MBD (methylated DNA binding domain) and TRD (transcription repression domain) (Figure 2A). In addition, a significant increase in intracellular MeCP2 content was detected in RPE cells treated with 20 ng/mL of human recombinant protein MeCP2 for 72 h, indicating that exogenous addition of MeCP2 can increase intracellular MeCP2 levels (Figure 2A). To elucidate the effect of MeCP2 treatment on gene expression in RPE cells, we performed transcriptome sequencing and analyzed differential genes. To select differentially expressed genes, we set the cutoff values of *p*-values and fold changes to 0.05 and 1.5, respectively. The volcano plot showed that 65 genes were up-regulated and 43 genes were down-regulated at the RNA level after MeCP2 induction, and each dot represented a gene (Figure 2B). The clustering heatmap marked with key genes revealed differential gene expression in 6 samples from two groups (Figure 2C).

Additionally, to clarify with which biological functions and pathways the DEGs are associated with, we annotated the functions of the DEGs by GO and KEGG analysis. As shown in Figure 2D, the DEGs were related to organic acid metabolic process (including fatty acid, long-chain fatty acid, and unsaturated fatty acid), some biological processes (cAMP biosynthesis, programmed cell death, and ion transport), and protein kinase C-activating G protein-coupled receptor signaling pathway. Genes involved in these biological functions mainly included *EDN1*, *PTGES*, *HTR1B*, *INHA*, and *ABCC11*. KEGG enrichment manifested that DEGs participated in renin secretion, melanogenesis, vascular smooth muscle contraction, AGE-RAGE signaling, cAMP signaling, and apelin signaling pathway (Figure 2E, Table S1). Genes participating in these biological pathways were mainly *PLCB2*, *EDN1*, *ORAI1*, and *EGR1*.

3.2. Characteristics of m6A Modification in hTERT RPE-1 Cells. m6A methylation is the most widespread internal modification of eukaryotic mRNA. To explore the modification profile of m6A in hTERT RPE-1 cells, we performed m6A sequencing and analyzed the m6A peaks. By m6A-seq, we detected 9,441 and 9,735 m6A peaks in the control and MeCP2 groups, corresponding to 7,199 and 7,333 genes (Figure 3A), respectively. In addition, 1,241 extra m6A peaks and 947 missing m6A peaks were found in the MeCP2 group, corresponding to 490 and 356 genes, respectively (Tables S2 and S3). By analyzing the distribution of m6A methylation across functional regions of transcripts, we found no significant difference between the control and MeCP2 groups, and the abundance of m6A modification was largest in introns, followed by 3′UTR and CDS regions (Figure 3B).

Homer software analyzed the common motifs among m6A peaks and drew the motif diagrams.[26] The results indicated that the RRACH motif was dominant in both the control and MeCP2 groups, accounting for 43.56 and 43.39% of the total target sequences, respectively (Figure 3C). Furthermore, by analyzing the distribution of m6A-modified transcripts in the corresponding chromosomes, we found that m6A-modified transcripts originated from all chromosomes except chromosome Y, which was attributed to the fact that hTERT RPE-1 cells were derived from females. In addition, there were 1,552

https://doi.org/10.1021/acsomega.3c06610
ACS Omega 2023, 8, 47964−47973

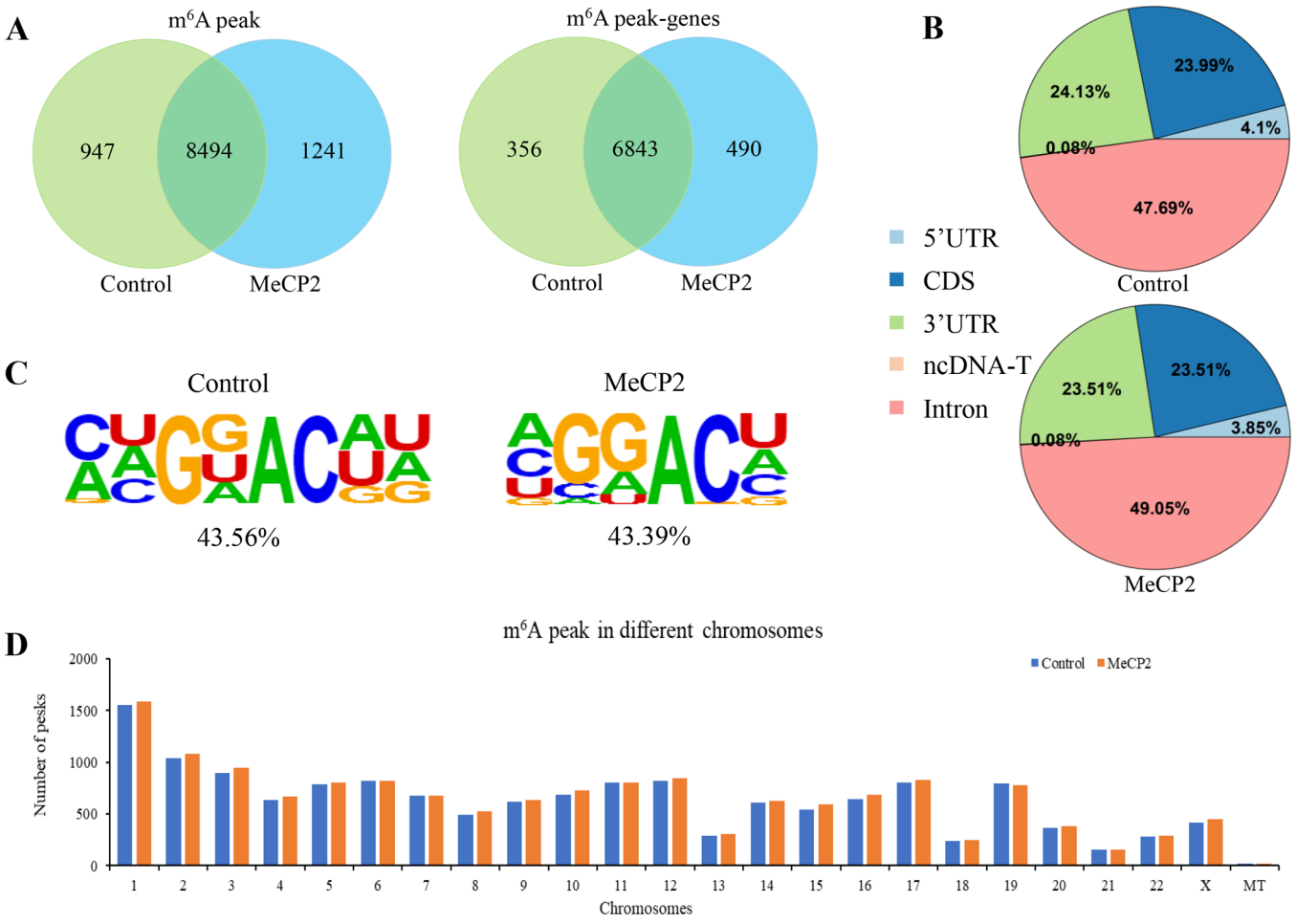

Figure 3. Characteristics of m6A modification in hTERT RPE-1 cells. (A) Overlapping peaks and overlapping genes are associated with m6A peaks in the control and MeCP2 groups. (B) Analysis of the m6A peak distribution in different transcript regions. ncDNA-T: transcript of noncoding DNA. (C) Analysis of the m6A motif and its proportion in the total target sequence. (D) Analysis of the distribution of m6A-modified transcripts on each corresponding chromosome.

and 1,588 peaks on chromosome 1 and 22 and 21 peaks on mitochondrial DNA in the control and MeCP2 groups, respectively (Figure 3D). However, there was no significant difference in the number of m6A-modified transcripts on each chromosome between the two groups.

3.3. Differentially Methylated Genes (DMGs) Induced by MeCP2 in hTERT RPE-1 Cells. In order to investigate the changes of m6A methylation abundance in each gene caused by MeCP2 treatment, we selected DMGs by setting the cutoff values of fold change (FC < 1.5) and false discovery rate (FDR < 0.05). Comparison of the control and MeCP2-treated groups revealed 9,041 down-regulated m6A peaks corresponding to 4,210 genes, as well as four up-regulated m6A peaks corresponding to *ZBTB40*,*ZNF93*, *ZNF283*, and *MAP7D2* genes (Figure 4A, Table S4). Among them, the *ZBTB40* gene contains one up-regulated m6A peak and one down-regulated m6A peak, which is a zinc finger protein associated with transcriptional regulation. We analyzed the DMGs distribution on each chromosome and discovered that the number of DMGs was the largest on chromosome 1, followed by chromosomes 2 and 19, and the number of mitochondrial DNA was the least (Figure 4B).

GO and KEGG enrichment further analyzed the DMGs function and showed that they were associated with RNA metabolism and binding, protein binding, nucleic acid transcription, and gene expression (Figure 4C). In addition, DMGs were also related to cell junction (adhesions junction, focal adhesion, and tight junction), RNA processing and metabolism (RNA degradation, spliceosome, ribosome biogenesis), cell activity (cell cycle and apoptosis), actin cytoskeleton, and several signaling pathways (MAPK, Wnt, Hippo, TNF, and AGE-RAGE pathway) (Figure 4D). Finally, Figure 4E shows the enrichment numbers of DMGs in different KEGG pathways, and 440 DMGs are involved in signal transduction.

3.4. Conjoint Analysis of DMGs and DEGs. Since m6A methylation plays critical roles in a variety of biological processes, such as RNA metabolism, alterations in m6A abundance have dramatic effects on the transcript levels. To discover which genes were altered in both m6A abundance and mRNA levels, we performed a conjoint analysis of DMGs and DEGs. Figure 5A reveals that three genes (*EGR1*, *ELOVL2*, and *SFR1*) were altered at the m6A and mRNA levels. In addition, we analyzed the distribution of m6A peaks in the transcripts of these genes and found that the m6A abundances of three genes were all down-regulated (Figure 5B–D). The *EGR1* gene contained four down-regulated m6A peaks, the *ELOVL2* gene contained one down-regulated m6A peak, and the *SFR1* gene contained two down-regulated m6A peaks (Table 1). However, the corresponding transcript levels

https://doi.org/10.1021/acsomega.3c06610
ACS Omega 2023, 8, 47964−47973

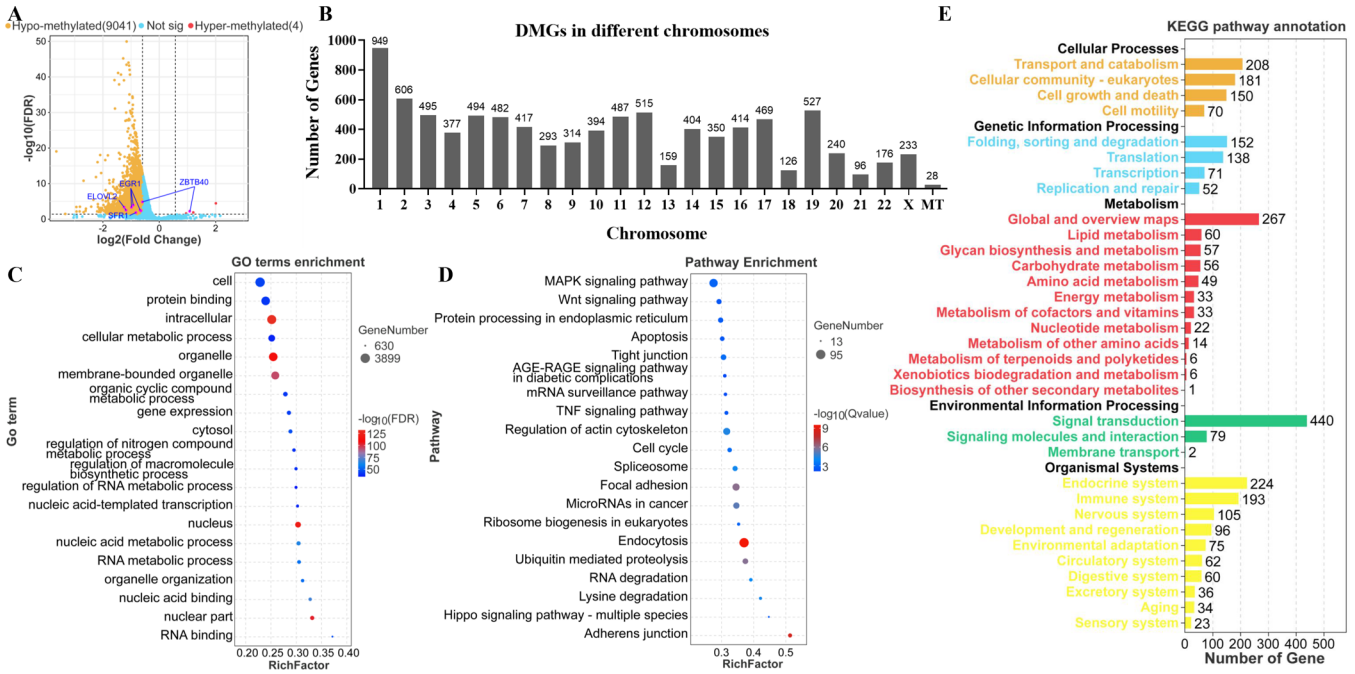

Figure 4. MeCP2-induced alterations in m6A methylation in hTERT RPE-1 cells. (A) Volcano plot of differentially methylated peaks. Each dot represents an m6A peak, with orange representing the hypomethylated peak and red representing the hypermethylated peak. (B). Analysis of DMGs distribution on each chromosome. GO enrichment (C) and KEGG enrichment (D) of DMGs. (E) Enrichment numbers of DMGs in different KEGG pathways. Black font indicates the KEGG A class, and colored font indicates the KEGG B class.

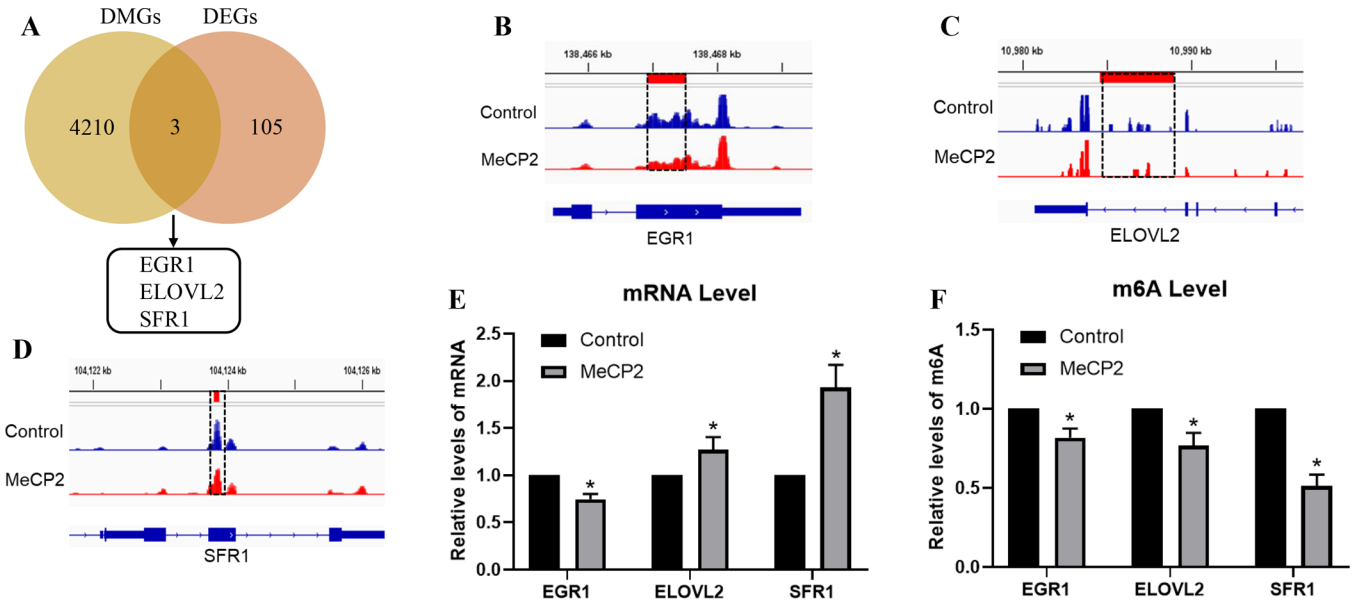

Figure 5. Conjoint Analysis of DMGs and DEGs. (A) Overlap of the DMGs and DEGs. The intersection included *EGR1*, *ELOVL2*, and *SFR1* genes. (B–D) IGV diagrams of m6A abundances in *EGR1*, *ELOVL2*, and *SFR1* transcripts. The dashed lines represent the region of the difference peaks. (E) qPCR validation of the mRNA level of *EGR1*, *ELOVL2*, and *SFR1* genes. (F) m6A-IP-qPCR validation of the m6A level of *EGR1*, *ELOVL2*, and *SFR1* transcripts. Asterisks indicate that the *p* value is less than 0.05 of the *t* test.

showed that *EGR1* was down-regulated, and *ELOVL2* and *SFR1* were up-regulated. We further verified the mRNA levels and m6A levels of these genes and found them to be consistent with the sequencing results (Figure 5E, F).

4. DISCUSSION

MeCP2 acts as a transcription factor, and its imbalance affects gene expression. Here, we first used RNA-seq to identify gene expression changes in RPE cells after treatment with the recombinant protein MeCP2, and we found that a total of 108 genes were altered in RNA levels (Figure 2B). Enrichment analysis exhibited that DEGs were related to fatty acid metabolism, renin secretion, vascular smooth muscle contraction, AGE-RAGE signaling, cAMP signaling, and apelin signaling pathway (Figure 2D,E). In these pathways, abnormal lipid metabolism is frequently associated with cancer cell invasion and migration by affecting energy metabolism related pathways.[30,31] The renin–angiotensin system affects the

https://doi.org/10.1021/acsomega.3c06610
ACS Omega 2023, 8, 47964–47973

Table 1. mRNA Levels and m6A Abundance of *EGR1*, *ELOVL2* and *SFR1* Genes

			mRNA		m6A		
gene ID	description	chromosome	logFC	*p*-value	logFC	FDR	annotation
EGR1	early growth response 1, transcriptional regulator	5	−0.6664	4.15×10^{-9}	−0.6398	5.47×10^{-3}	CDS
					−0.9130	1.41×10^{-4}	CDS
					−0.6677	3.51×10^{-3}	CDS
					−0.9759	5.72×10^{-4}	CDS
ELOVL2	ELOVL fatty acid elongase 2	6	0.6091	0.0350	−1.2376	5.16×10^{-4}	3′UTR
SFR1	SWI5 dependent homologous recombination repair protein 1	10	0.6641	0.0033	−0.8193	0.0173	CDS
					−1.1687	3.63×10^{-3}	CDS

function of vascular smooth muscle, which is closely related to hypertension, cardiomyopathy, and chronic kidney disease,[32,33] suggesting that MeCP2 might be involved in various diseases. Additionally, the AGE-RAGE pathway exhibits inhibitory effects on EMT and pulmonary fibrosis by upregulating Smad7 expression.[34] The cAMP signaling pathway controls multiple physiological processes such as metabolism, muscle contraction, and gene transcription and is involved in suppressing the EMT process induced by TGF-β1.[35,36] The apelin signaling pathway is associated with renal fibrosis and inhibits the EMT process by regulating the SMAD pathway.[37,38] These results suggest that imbalanced expression levels of MeCP2 affect multiple cellular pathways that regulate the EMT process.

Moreover, the DEGs involved in these biological functions mainly include *EDN1*, *PTGES*, *HTR1B*, *INHA*, *ABCC11*, *PLCB2*, *ORAI1*, and *EGR1*, which encode endothelin-1, prostaglandin E synthase, 5-hydroxytryptamine receptor 1B, inhibin alpha chain, ATP-binding cassette subfamily C member 11, phospholipase C β2, ORAI calcium release-activated calcium modulator 1, and early growth response 1, respectively. Among them, *EDN1* promotes RPE cell proliferation, migration, and extracellular matrix molecule (ECM) secretion through Akt/Erk signaling pathways and plays crucial roles in the development of PVR.[39] *PTGES* is involved in the synthesis of prostaglandin E2 (PGE2), and its expression is highly correlated with inflammation and cancer.[40] *PLCB2* is associated with the melanoma growth, and knockdown of *PLCB2* inhibits cell activity and facilitates apoptosis by activating the Ras/Raf/MAPK signaling pathway.[41] ORAI1-mediated calcium (Ca^{2+}) channels controls key events in cancer cells, including cell proliferation, invasion, and resistance.[42] The above genes may be the entry points for the connection between MeCP2 and the EMT process.

We further performed m6A-seq and found that m6A methylation preferentially recognized RRACH motifs and was abundant in the 3′UTR and intron regions (Figure 3B), which was consistent with previous studies.[43] Because hTERT RPE-1 cells were female in origin, m6A-seq failed to detect m6A peaks derived from chromosome Y. This suggests that gender may be a factor in the EMT process of RPE cells. Some studies have found that female sex hormones inhibit TGF-β2-induced collagen contraction in RPE cells by suppressing the expression of MMP, α-SMA, and fibronectin. In addition, both estrogen receptor (ER) and progesterone receptor (PR) are significantly expressed on the PVR membrane.[44] Studies have also found that gender factors affect the expression of EMT key genes (such as SNAI1/2, ZEB1, and DDR1) in cancer cells, thereby affecting cancer progression, especially liver cancer.[45,46] However, there are currently few studies on the correlation between gender factors and the EMT process of RPE cells. By comparing the m6A methylation difference between the control and MeCP2 groups, we discovered that the m6A abundance of most DMGs was down-regulated in the MeCP2 group (Figure 4A). This suggests that MeCP2 may induce hypomethylation of a large number of genes. Enrichment analysis found that DMGs were associated with cell junction, RNA processing and metabolism, cell activity, actin cytoskeleton, and diverse signaling pathways (Figure 4D). Among them, adhesions junctions and tight junctions play essential roles in maintaining the structural integrity and homeostasis of epithelial cells.[47] Focal adhesion serves as anchoring units between cells and the extracellular matrix and is involved in cell differentiation, proliferation, migration, and cell cycle.[48] Due to the altered or absent cell junctions, cells lose their epithelial properties and undergo the EMT process. DMGs were also enriched in RNA processing and metabolic pathways, suggesting that MeCP2 may be involved in the post-transcriptional regulation of gene expression through m6A methylation. In addition, mesenchymal cells exhibit enhanced migratory capacity, and the actin cytoskeleton may be a contributor to this process.[49] Moreover, MAPK, Wnt, Hippo, and TNF signaling pathways have all been shown to be involved in regulating the EMT process,[50−53] indicating that MeCP2-induced alternations may mobilize multiple signaling pathways in m6A-dependent manners.

In addition, we found that *EGR1*, *ELOVL2* and *SFR1* genes were altered at the m6A level and RNA level (Table 1). Among them, EGR1 has been extensively studied as a key transcription factor. It is expressed in a variety of cell types and is closely associated with some important physiological processes such as cell differentiation, proliferation, apoptosis, and invasion and is involved in tissue damage, immune response, and fibrosis.[54] In addition, the role of the transcription factor EGR1 in EMT has also been revealed, although its function in RPE cells is unknown. Studies have shown that the EGR1 expression is decreased in lung cancer primary cells after stimulation with TGF-β1, and overexpression of EGR1 attenuated TGF-β1-enhanced cell migration ability.[55] Moreover, EGR1 is down-regulated in bladder cancer tissues compared with adjacent normal tissues, and increased EGR1 expression inhibits cell migration, proliferation, and invasiveness.[56] Furthermore, in breast cancer, the EGR1 expression is positively correlated with its target gene frizzled-related protein (FRZB), both of which are lowly expressed in cancer tissue, and FRZB further inhibits cell growth and invasion.[57] The function of ELOVL2 in cancers is also emerging. ELOVL2 is involved in the fatty acids elongation and is highly expressed in renal cell carcinoma.[58] However, the relationship between SFR1 (participated in homologous recombination repair) and EMT has not been revealed. Based on the above results, we

https://doi.org/10.1021/acsomega.3c06610
ACS Omega 2023, 8, 47964−47973

speculated that EGR1 might play crucial roles in the MeCP2-induced phenotype through m6A methylation.

Our results showed that treatment of RPE cells with MeCP2 downregulated m6A abundance and RNA levels of the transcription factor EGR1. Based on the function of EGR1 in EMT and fibrosis, we speculate that reduced m6A abundance of EGR1 transcripts in RPE cells results in downregulation of its RNA and protein levels. We further speculate that EGR1 may participate in the pathogenesis of PVR. However, the mechanism by which MeCP2 affects m6A modification remains to be further explored. It was shown that MeCP2 is able to competitively bind to methyltransferase METTL14, thereby affecting the function of METTL14.[13] So, in RPE cells, does MeCP2 affect the m6A abundance of EGR1 by affecting methyltransferase function through competitive binding to methyltransferases or by inhibiting methyltransferase expression through its transcriptional repressive activity? Including the function of EGR1 in the EMT of RPE cells and PVR processes, these questions need to be further investigated. Furthermore, as mentioned above, gender may be a factor that affects EMT of RPE cells in m6A manners, since m6A modifications may also be present on transcripts originating from chromosome Y. Therefore, whether chromosome Y-derived m6A-modified transcripts affect EMT and PVR processes remains to be explored in depth.

In conclusion, this study revealed the pattern of m6A modification in hTERT RPE-1 cells and identified changes in the abundance of m6A modifications of individual genes after MeCP2 treatment. Combined with RNA expression differences, *EGR1*, *ELOVL2*, and *SFR1* genes were altered at the RNA level and m6A level, suggesting that these genes might be involved in MeCP2 regulation in an m6A-dependent manner.

■ ASSOCIATED CONTENT

Data Availability Statement

The data in this study is included in the article. Raw data from sequencing has been uploaded to the SRA database (SRA accession: SRP470199, Bioproject: PRJNA1035791).

Supporting Information

The Supporting Information is available free of charge at https://pubs.acs.org/doi/10.1021/acsomega.3c06610.

Annotated differentially expressed genes, annotated peaks in the control group, annotated peaks in the MeCP2 group, and annotated differentially methylated genes (PDF)

■ AUTHOR INFORMATION

Corresponding Author

Xiaohua Li − *Henan Eye Hospital, Henan Key Laboratory of Ophthalmology and Visual Science, Henan Provincial People's Hospital, Zhengzhou 450003, China; Zhengzhou University People's Hospital, 450000 Zhengzhou, China; People's Hospital of Henan University, 450003 Zhengzhou, China; Eye Institute, Henan Academy of Innovations in Medical Science, 450000 Zhengzhou, China;* orcid.org/0000-0001-5183-8055; Email: xhl_6116@163.com

Authors

Xueru Zhao − *Henan Eye Hospital, Henan Key Laboratory of Ophthalmology and Visual Science, Henan Provincial People's Hospital, Zhengzhou 450003, China; Zhengzhou University People's Hospital, 450000 Zhengzhou, China; People's Hospital of Henan University, 450003 Zhengzhou, China; Eye Institute, Henan Academy of Innovations in Medical Science, 450000 Zhengzhou, China*

Yongya Zhang − *Henan Eye Hospital, Henan Key Laboratory of Ophthalmology and Visual Science, Henan Provincial People's Hospital, Zhengzhou 450003, China; Zhengzhou University People's Hospital, 450000 Zhengzhou, China*

Fei Wu − *Henan Eye Hospital, Henan Key Laboratory of Ophthalmology and Visual Science, Henan Provincial People's Hospital, Zhengzhou 450003, China; Zhengzhou University People's Hospital, 450000 Zhengzhou, China*

Xue Li − *Henan Eye Hospital, Henan Key Laboratory of Ophthalmology and Visual Science, Henan Provincial People's Hospital, Zhengzhou 450003, China; Zhengzhou University People's Hospital, 450000 Zhengzhou, China; People's Hospital of Henan University, 450003 Zhengzhou, China; Eye Institute, Henan Academy of Innovations in Medical Science, 450000 Zhengzhou, China*

Sibei Guo − *Henan Eye Hospital, Henan Key Laboratory of Ophthalmology and Visual Science, Henan Provincial People's Hospital, Zhengzhou 450003, China; Xinxiang Medical University Henan Provincial People's Hospital, 453003 Xinxiang, China*

Complete contact information is available at: https://pubs.acs.org/10.1021/acsomega.3c06610

Author Contributions

X.H.L. designed the research and provided advice on supervision. X.R.Z. wrote the manuscript. Y.Y.Z., F.W., X.L., and S.B.G. performed the experiments. X.R.Z. conducted the data analysis. All authors contributed to editorial changes in the manuscript. All authors read and approved the final manuscript.

Funding

This study was funded by National Natural Science Foundation of China (81770952).

Notes

No potential conflicts of interest were disclosed.
The authors declare no competing financial interest.

■ REFERENCES

(1) Zhou, M.; Geathers, J. S.; Grillo, S. L.; Weber, S. R.; Wang, W.; Zhao, Y.; Sundstrom, J. M. Role of Epithelial-Mesenchymal Transition in Retinal Pigment Epithelium Dysfunction. *Front Cell Dev Biol.* **2020**, *8*, 501.

(2) Zou, H.; Shan, C.; Ma, L.; Liu, J.; Yang, N.; Zhao, J. Polarity and epithelial-mesenchymal transition of retinal pigment epithelial cells in proliferative vitreoretinopathy. *PeerJ.* **2020**, *8*, No. e10136.

(3) Jerdan, J. A.; Pepose, J. S.; Michels, R. G.; Hayashi, H.; de Bustros, S.; Sebag, M.; Glaser, B. M. Proliferative vitreoretinopathy membranes. An immunohistochemical study. *Ophthalmology* **1989**, *96* (6), 801−810.

(4) Bhatt, A. B.; Patel, S.; Matossian, M. D.; Ucar, D. A.; Miele, L.; Burow, M. E.; Flaherty, P. T.; Cavanaugh, J. E. Molecular Mechanisms of Epithelial to Mesenchymal Transition Regulated by ERK5 Signaling. *Biomolecules.* **2021**, *11* (2), 183.

(5) Zaccara, S.; Ries, R. J.; Jaffrey, S. R. Reading, writing and erasing mRNA methylation. *Nat. Rev. Mol. Cell Biol.* **2019**, *20* (10), 608−624.

(6) Li, X.; Ma, B.; Zhang, W.; Song, Z.; Zhang, X.; Liao, M.; Li, X.; Zhao, X.; Du, M.; Yu, J.; He, S.; Yan, H. The essential role of N6-methyladenosine RNA methylation in complex eye diseases. *Genes & diseases.* **2023**, *10* (2), 505−520.

(7) Ma, X.; Long, C.; Wang, F.; Lou, B.; Yuan, M.; Duan, F.; Yang, Y.; Li, J.; Qian, X.; Zeng, J.; Lin, S.; Shen, H.; Lin, X. METTL3

attenuates proliferative vitreoretinopathy and epithelial-mesenchymal transition of retinal pigment epithelial cells via wnt/β-catenin pathway. *Journal of cellular and molecular medicine.* **2021**, *25* (9), 4220−4234.
(8) Wang, Y.; Chen, Y.; Liang, J.; Jiang, M.; Zhang, T.; Wan, X.; Wu, J.; Li, X.; Chen, J.; Sun, J.; Hu, Y.; Huang, P.; Feng, J.; Liu, T.; Sun, X. METTL3-mediated m6A modification of HMGA2 mRNA promotes subretinal fibrosis and epithelial-mesenchymal transition. *J. Mol. Cell Biol.* **2023**, mjad005 DOI: 10.1093/jmcb/mjad005.
(9) Cao, G.; Li, H. B.; Yin, Z.; Flavell, R. A. Recent advances in dynamic m6A RNA modification. *Open biology.* **2016**, *6* (4), No. 160003.
(10) Adkins, N. L.; Georgel, P. T. MeCP2: structure and function. *Biochem. Cell Biol.* **2011**, *89* (1), 1−11.
(11) Magdinier, F.; Billard, L. M.; Wittmann, G.; Frappart, L.; Benchaïb, M.; Lenoir, G. M.; Guérin, J. F.; Dante, R. Regional methylation of the 5′ end CpG island of BRCA1 is associated with reduced gene expression in human somatic cells. *Faseb j.* **2000**, *14* (11), 1585−1594.
(12) Chen, T.; Cai, S. L.; Li, J.; Qi, Z. P.; Li, X. Q.; Ye, L. C.; Xie, X. F.; Hou, Y. Y.; Yao, L. Q.; Xu, M. D.; Zhou, P. H.; Xu, J. M.; Zhong, Y. S. Mecp2-mediated Epigenetic Silencing of miR-137 Contributes to Colorectal Adenoma-Carcinoma Sequence and Tumor Progression via Relieving the Suppression of c-Met. *Scientific reports.* **2017**, *7*, 44543.
(13) Wang, S.; Gan, M.; Chen, C.; Zhang, Y.; Kong, J.; Zhang, H.; Lai, M. Methyl CpG binding protein 2 promotes colorectal cancer metastasis by regulating N(6) -methyladenosine methylation through methyltransferase-like 14. *Cancer science.* **2021**, *112* (8), 3243−3254.
(14) Nan, X.; Ng, H. H.; Johnson, C. A.; Laherty, C. D.; Turner, B. M.; Eisenman, R. N.; Bird, A. Transcriptional repression by the methyl-CpG-binding protein MeCP2 involves a histone deacetylase complex. *Nature.* **1998**, *393* (6683), 386−389.
(15) Chahrour, M.; Jung, S. Y.; Shaw, C.; Zhou, X.; Wong, S. T.; Qin, J.; Zoghbi, H. Y. MeCP2, a key contributor to neurological disease, activates and represses transcription. *Science.* **2008**, *320* (5880), 1224−1229.
(16) Amir, R. E.; Van den Veyver, I. B.; Wan, M.; Tran, C. Q.; Francke, U.; Zoghbi, H. Y. Rett syndrome is caused by mutations in X-linked MECP2, encoding methyl-CpG-binding protein 2. *Nat. Genet.* **1999**, *23* (2), 185−188.
(17) Jiang, W.; Liang, Y. L.; Liu, Y.; Chen, Y. Y.; Yang, S. T.; Li, B. R.; Yu, Y. X.; Lyu, Y.; Wang, R. MeCP2 inhibits proliferation and migration of breast cancer via suppression of epithelial-mesenchymal transition. *Journal of cellular and molecular medicine.* **2020**, *24* (14), 7959−7967.
(18) Wang, H.; Li, J.; He, J.; Liu, Y.; Feng, W.; Zhou, H.; Zhou, M.; Wei, H.; Lu, Y.; Peng, W.; Du, F.; Gong, A.; Xu, M. Methyl-CpG-binding protein 2 drives the Furin/TGF-β1/Smad axis to promote epithelial-mesenchymal transition in pancreatic cancer cells. *Oncogenesis.* **2020**, *9* (8), 76.
(19) He, S.; Barron, E.; Ishikawa, K.; Nazari Khanamiri, H.; Spee, C.; Zhou, P.; Kase, S.; Wang, Z.; Dustin, L. D.; Hinton, D. R. Inhibition of DNA Methylation and Methyl-CpG-Binding Protein 2 Suppresses RPE Transdifferentiation: Relevance to Proliferative Vitreoretinopathy. *Investigative ophthalmology & visual science.* **2015**, *56* (9), 5579−5589.
(20) Li, X.; Li, X.; He, S.; Zhao, M. MeCP2−421-mediated RPE epithelial-mesenchymal transition and its relevance to the pathogenesis of proliferative vitreoretinopathy. *Journal of cellular and molecular medicine.* **2020**, *24* (16), 9420−9427.
(21) Dominissini, D.; Moshitch-Moshkovitz, S.; Salmon-Divon, M.; Amariglio, N.; Rechavi, G. Transcriptome-wide mapping of N(6)-methyladenosine by m(6)A-seq based on immunocapturing and massively parallel sequencing. *Nat. Protoc.* **2013**, *8* (1), 176−189.
(22) Modi, A.; Vai, S.; Caramelli, D.; Lari, M. The Illumina Sequencing Protocol and the NovaSeq 6000 System. *Methods Mol. Biol.* **2021**, *2242*, 15−42.
(23) Ma, K. Y.; He, C.; Wendel, B. S.; Williams, C. M.; Xiao, J.; Yang, H.; Jiang, N. Immune Repertoire Sequencing Using Molecular Identifiers Enables Accurate Clonality Discovery and Clone Size Quantification. *Front Immunol.* **2018**, *9*, 33.
(24) Meng, J.; Cui, X.; Rao, M. K.; Chen, Y.; Huang, Y. Exome-based analysis for RNA epigenome sequencing data. *Bioinformatics.* **2013**, *29* (12), 1565−1567.
(25) Ramirez, F.; Ryan, D. P.; Gruning, B.; Bhardwaj, V.; Kilpert, F.; Richter, A. S.; Heyne, S.; Dundar, F.; Manke, T. deepTools2: a next generation web server for deep-sequencing data analysis. *Nucleic Acids Res.* **2016**, *44* (W1), W160−W165.
(26) Heinz, S.; Benner, C.; Spann, N.; Bertolino, E.; Lin, Y. C.; Laslo, P.; Cheng, J. X.; Murre, C.; Singh, H.; Glass, C. K. Simple combinations of lineage-determining transcription factors prime cis-regulatory elements required for macrophage and B cell identities. *Mol. Cell* **2010**, *38* (4), 576−589.
(27) Robinson, M. D.; McCarthy, D. J.; Smyth, G. K. edgeR: a Bioconductor package for differential expression analysis of digital gene expression data. *Bioinformatics.* **2010**, *26* (1), 139−140.
(28) Wang, S.; Su, W.; Zhong, C.; Yang, T.; Chen, W.; Chen, G.; Liu, Z.; Wu, K.; Zhong, W.; Li, B.; Mao, X.; Lu, J. An Eight-CircRNA Assessment Model for Predicting Biochemical Recurrence in Prostate Cancer. *Front Cell Dev Biol.* **2020**, *8*, No. 599494.
(29) Thorvaldsdottir, H.; Robinson, J. T.; Mesirov, J. P. Integrative Genomics Viewer (IGV): high-performance genomics data visualization and exploration. *Brief Bioinform.* **2013**, *14* (2), 178−192.
(30) Tian, W.; Zhang, W.; Zhang, Y.; Zhu, T.; Hua, Y.; Li, H.; Zhang, Q.; Xia, M. FABP4 promotes invasion and metastasis of colon cancer by regulating fatty acid transport. *Cancer Cell Int.* **2020**, *20*, 512.
(31) Wang, M. D.; Wang, N. Y.; Zhang, H. L.; Sun, L. Y.; Xu, Q. R.; Liang, L.; Li, C.; Huang, D. S.; Zhu, H.; Yang, T. Fatty acid transport protein-5 (FATP5) deficiency enhances hepatocellular carcinoma progression and metastasis by reprogramming cellular energy metabolism and regulating the AMPK-mTOR signaling pathway. *Oncogenesis.* **2021**, *10* (11), 74.
(32) Touyz, R. M.; Alves-Lopes, R.; Rios, F. J.; Camargo, L. L.; Anagnostopoulou, A.; Arner, A.; Montezano, A. C. Vascular smooth muscle contraction in hypertension. *Cardiovascular research.* **2018**, *114* (4), 529−539.
(33) Tao, H.; Tao, J. Y.; Song, Z. Y.; Shi, P.; Wang, Q.; Deng, Z. Y.; Ding, X. S. MeCP2 triggers diabetic cardiomyopathy and cardiac fibroblast proliferation by inhibiting RASSF1A. *Cell Signal.* **2019**, *63*, No. 109387.
(34) Song, J. S.; Kang, C. M.; Park, C. K.; Yoon, H. K.; Lee, S. Y.; Ahn, J. H.; Moon, H. S. Inhibitory effect of receptor for advanced glycation end products (RAGE) on the TGF-β-induced alveolar epithelial to mesenchymal transition. *Experimental & molecular medicine.* **2011**, *43* (9), 517−524.
(35) Schmidt, M.; Dekker, F. J.; Maarsingh, H. Exchange protein directly activated by cAMP (epac): a multidomain cAMP mediator in the regulation of diverse biological functions. *Pharmacological reviews.* **2013**, *65* (2), 670−709.
(36) Zuo, H.; Trombetta-Lima, M.; Heijink, I. H.; van der Veen, C.; Hesse, L.; Faber, K. N.; Poppinga, W. J.; Maarsingh, H.; Nikolaev, V. O.; Schmidt, A. M. A-Kinase Anchoring Proteins Diminish TGF-β(1)/Cigarette Smoke-Induced Epithelial-To-Mesenchymal Transition. *Cells.* **2020**, *9* (2), 356.
(37) Wang, L. Y.; Diao, Z. L.; Zhang, D. L.; Zheng, J. F.; Zhang, Q. D.; Ding, J. X.; Liu, W. H. The regulatory peptide apelin: a novel inhibitor of renal interstitial fibrosis. *Amino acids.* **2014**, *46* (12), 2693−2704.
(38) Wang, L. Y.; Diao, Z. L.; Zheng, J. F.; Wu, Y. R.; Zhang, Q. D.; Liu, W. H. Apelin attenuates TGF-β1-induced epithelial to mesenchymal transition via activation of PKC-ε in human renal tubular epithelial cells. *Peptides.* **2017**, *96*, 44−52.
(39) Qin, D.; Zhang, L.; Jin, X.; Zhao, Z.; Jiang, Y.; Meng, Z. Effect of Endothelin-1 on proliferation, migration and fibrogenic gene expression in human RPE cells. *Peptides.* **2017**, *94*, 43−48.

(40) Wang, T.; Jing, B.; Xu, D.; Liao, Y.; Song, H.; Sun, B.; Guo, W.; Xu, J.; Li, K.; Hu, M.; Liu, S.; Ling, J.; Kuang, Y.; Zhang, T.; Zhang, S.; Yao, F.; Zhou, B. P.; Deng, J. PTGES/PGE(2) signaling links immunosuppression and lung metastasis in Gprc5a-knockout mouse model. *Oncogene.* **2020**, *39* (15), 3179−3194.
(41) Zhang, H.; Xie, T.; Shui, Y.; Qi, Y. Knockdown of PLCB2 expression reduces melanoma cell viability and promotes melanoma cell apoptosis by altering Ras/Raf/MAPK signals. *Molecular medicine reports.* **2019**, *21* (1), 420−428.
(42) Chalmers, S. B.; Monteith, G. R. ORAI channels and cancer. *Cell calcium.* **2018**, *74*, 160−167.
(43) Zhang, C.; Chen, Y.; Sun, B.; Wang, L.; Yang, Y.; Ma, D.; Lv, J.; Heng, J.; Ding, Y.; Xue, Y.; Lu, X.; Xiao, W.; Yang, Y. G.; Liu, F. m(6)A modulates haematopoietic stem and progenitor cell specification. *Nature.* **2017**, *549* (7671), 273−276.
(44) Kimura, K.; Orita, T.; Fujitsu, Y.; Liu, Y.; Wakuta, M.; Morishige, N.; Suzuki, K.; Sonoda, K. H. Inhibition by female sex hormones of collagen gel contraction mediated by retinal pigment epithelial cells. *Investigative ophthalmology & visual science.* **2014**, *55* (4), 2621−2630.
(45) Kim, S. Y.; Lee, S.; Lee, E.; Lim, H.; Shin, J. Y.; Jung, J.; Kim, S. G.; Moon, A. Sex-biased differences in the correlation between epithelial-to-mesenchymal transition-associated genes in cancer cell lines. *Oncology letters.* **2019**, *18* (6), 6852−6868.
(46) Song, H. K.; Kim, S. Y. Gender Disparity of EMT-related Gene Expression Affects Survival of Hepatocellular Carcinoma Patients. *Yakhak Hoeji.* **2019**, *63* (6), 390−398.
(47) Yu, Y.; Elble, R. C. Homeostatic Signaling by Cell-Cell Junctions and Its Dysregulation during Cancer Progression. *Journal of clinical medicine.* **2016**, *5* (2), 26.
(48) Mishra, Y. G.; Manavathi, B. Focal adhesion dynamics in cellular function and disease. *Cell Signal.* **2021**, *85*, No. 110046.
(49) Merino, F.; Pospich, S.; Raunser, S. Towards a structural understanding of the remodeling of the actin cytoskeleton. *Semin Cell Dev Biol.* **2020**, *102*, 51−64.
(50) Zavadil, J.; Bitzer, M.; Liang, D.; Yang, Y. C.; Massimi, A.; Kneitz, S.; Piek, E.; Bottinger, E. P. Genetic programs of epithelial cell plasticity directed by transforming growth factor-beta. *Proc. Natl. Acad. Sci. U. S. A.* **2001**, *98* (12), 6686−6691.
(51) Chen, H. C.; Zhu, Y. T.; Chen, S. Y.; Tseng, S. C. Wnt signaling induces epithelial-mesenchymal transition with proliferation in ARPE-19 cells upon loss of contact inhibition. *Laboratory investigation; a journal of technical methods and pathology.* **2012**, *92* (5), 676−687.
(52) Lei, Q. Y.; Zhang, H.; Zhao, B.; Zha, Z. Y.; Bai, F.; Pei, X. H.; Zhao, S.; Xiong, Y.; Guan, K. L. TAZ promotes cell proliferation and epithelial-mesenchymal transition and is inhibited by the hippo pathway. *Mol. Cell. Biol.* **2008**, *28* (7), 2426−2436.
(53) Bates, R. C.; Mercurio, A. M. Tumor necrosis factor-alpha stimulates the epithelial-to-mesenchymal transition of human colonic organoids. *Mol. Biol. Cell* **2003**, *14* (5), 1790−1800.
(54) Wang, B.; Guo, H.; Yu, H.; Chen, Y.; Xu, H.; Zhao, G. The Role of the Transcription Factor EGR1 in Cancer. *Frontiers in oncology.* **2021**, *11*, No. 642547.
(55) Shan, L. N.; Song, Y. G.; Su, D.; Liu, Y. L.; Shi, X. B.; Lu, S. J. Early Growth Response Protein-1 Involves in Transforming Growth factor-β1 Induced Epithelial-Mesenchymal Transition and Inhibits Migration of Non-Small-Cell Lung Cancer Cells. *Asian Pacific journal of cancer prevention: APJCP.* **2015**, *16* (9), 4137−4142.
(56) Yan, L.; Wang, Y.; Liang, J.; Liu, Z.; Sun, X.; Cai, K. MiR-301b promotes the proliferation, mobility, and epithelial-to-mesenchymal transition of bladder cancer cells by targeting EGR1. *Biochem. Cell Biol.* **2017**, *95* (5), 571−577.
(57) Liu, H.; Mei, Y.; Ma, X.; Zhang, X.; Nie, W. FRZB is Regulated by the Transcription Factor EGR1 and Inhibits the Growth and Invasion of Triple-Negative Breast Cancer Cells by Regulating the JAK/STAT3 Pathway. *Clinical breast cancer.* **2022**, *22* (7), 690−698.
(58) Tanaka, K.; Kandori, S.; Sakka, S.; Nitta, S.; Tanuma, K.; Shiga, M.; Nagumo, Y.; Negoro, H.; Kojima, T.; Mathis, B. J.; Shimazui, T.; Watanabe, M.; Sato, T. A.; Miyamoto, T.; Matsuzaka, T.; Shimano, H.; Nishiyama, H. ELOVL2 promotes cancer progression by inhibiting cell apoptosis in renal cell carcinoma. *Oncology reports.* **2021**, *47* (2), 23.

https://doi.org/10.1021/acsomega.3c06610
ACS Omega 2023, 8, 47964−47973